Articles in PresS. J Neurophysiol (October 1, 2014). doi:10.1152/jn.00531.2014

INFLUENCE OF COMMON SYNAPTIC INPUT TO MOTOR NEURONS ON THE NEURAL DRIVE TO MUSCLE IN ESSENTIAL TREMOR

Juan A. Gallego[1], Jakob L. Dideriksen[2], Ales Holobar[3], Jaime Ibáñez[4], José L. Pons[4],
Elan D. Louis[5], Eduardo Rocon[1,6], Dario Farina[2]

1. Neuroengineering and Cognitive Science Group, Centre for Automation and Robotics, Consejo Superior de Investigaciones Científicas, 28500 Arganda del Rey, Spain.

2. Department of Neurorehabilitation Engineering, Bernstein Focus Neurotechnology Göttingen, Bernstein Center for Computational Neuroscience, University Medical Center Göttingen, Georg-August University, 37075 Göttingen, Germany.

3. Faculty of Electrical Engineering and Computer Science, University of Maribor, 2000 Maribor, Slovenia.

4. Neural Rehabilitation Group, Cajal Institute, Consejo Superior de Investigaciones Científicas, 28002, Madrid, Spain.

5. Department of Neurology, College of Physicians and Surgeons, and Department of Epidemiology, Mailman School of Public Health, Columbia University, 10032 New York, New York, USA.

6. Post-graduate Program, Universidade Federal do Espírito Santo, 29075-910, Vitória, Brazil.

RUNNING HEAD: Neural Drive to Muscle in Essential Tremor

CORRESPONDENCE TO: Prof. Dario Farina, Bernstein Focus Neurotechnology Göttingen, Department of Neurorehabilitation Engineering, Universitätsmedizin, Georg-August-Universität Göttingen, Von-Siebold-Str. 4, 37075 Göttingen. Germany. E-mail: dario.farina@bccn.uni-goettingen.de. Phone: + 49 (0) 551 / 3920100. Fax: + 49 (0) 551 / 3920110.

ABSTRACT:

Tremor in essential tremor (ET) is generated by pathological oscillations at 4 to 12 Hz, likely originating at cerebello-thalamo-cortical pathways. However, the way in which tremor is represented in the output of the spinal cord circuitries is largely unknown because of the difficulties in identifying the behavior of individual motor units from tremulous muscles. By using novel methods for the decomposition of multichannel surface EMG, we provide a systematic analysis of the discharge properties of motor units in 9 ET patients, with concurrent recordings of EEG activity. This analysis allowed inferring the contribution of common synaptic inputs to motor neurons in ET. Motor unit short-term synchronization was significantly greater in ET patients than in healthy subjects. Further, the strong association between the degree of synchronization and the peak in coherence between motor unit spike trains at the tremor frequency indicated that the high synchronization levels were generated mainly by common synaptic inputs specifically at the tremor frequency. The coherence between EEG and motor unit spike trains demonstrated the presence of common cortical input to the motor neurons at the tremor frequency. Nonetheless, the strength of this input was uncorrelated to the net common synaptic input at the tremor frequency, suggesting a contribution of spinal afferents or secondary supraspinal pathways in projecting common input at the tremor frequency. These results provide the first systematic analysis of the neural drive to the muscle in ET and elucidate some of its characteristics that determine the pathological tremulous muscle activity.

KEYWORDS: pathological tremor, motor unit, motor neuron, coherence, EMG, EEG.

Introduction

Essential tremor (ET) is characterized by 4–12 Hz upper limb tremor during posture and movement (Benito-León and Louis. 2006). Tremor in ET is ultimately generated by the abnormal rhythmic entrainment of motor neurons innervating the affected muscles (Elble and Deuschl, 2009), which results from the combination of central oscillatory activity (at cerebello-thalamo-cortical pathways and possibly other structures; Benito-León and Louis, 2006), reflex loops with different arc length, and limb properties (McAuley and Marsden, 2000; Deuschl et al., 2001). The manner in which these mechanisms interact to generate the abnormal neural activity is not fully understood (Louis et al., 2013), partly because of the difficulty in directly recording the output of spinal motor neurons activating the tremulous muscles (neural drive to muscles).

Motor unit spike trains have been traditionally analyzed using intramuscular electrodes, a technique that suffers from several limitations, especially when applied in pathological conditions such as tremor. One of these limitations is the small number of identified motor units, which often does not comprise a representative sample of the active population (Merletti and Farina, 2009). Moreover, the invasiveness of the technique and the sensitivity to small electrode movements strongly limit its applicability in the investigation of tremor. Indeed, only one study, to our knowledge, has reported motor neuron discharge properties in ET using this technique (Elek et al., 1991), focusing on the tendency of individual motor neurons to fire paired or tripled discharges with short interspike epochs (ISI; ~10–90 ms). These paired discharges likely occur due to the presence of a large excitatory drive (Kudina and Andreeva, 2013) and are thus etiologically different to double discharges or doublets, which arise during delayed depolarization (Kudina and Andreeva, 2013) and have briefer ISIs (< 10 ms; Heckman and Enoka, 2012).

Despite the lack of direct measurements of motor unit behavior in tremor, there are long-standing assumptions on some of the motor unit properties in ET. For example, it is generally assumed that motor units in ET patients are highly synchronized (Elble and Deuschl, 2009), although this assumption has never been experimentally verified. If confirmed, the presence of high synchronization among motor units would imply high levels of common synaptic inputs to motor neurons, which may have cortical (Farmer et al., 1993), subcortical (Boonstra et al., 2008), or afferent origin (Dartnall et al., 2008).

In this study, we provide a systematic analysis of the discharge properties of motor units in ET patients, with concurrent recordings of EEG activity. Spike trains of individual motor units were identified using a novel algorithm for decomposing multi-channel surface EMG (Holobar et al., 2012), which permitted to reliably detect several motor units accurately and non-invasively. The availability of this technique provides the unique possibility to precisely assess for the first time the neural drive to muscle in ET. With this approach we aimed to first directly measure the levels of motor neuron synchronization in ET and to further investigate the strength and source of common synaptic inputs to the motor neuron pool using coherence analysis, both between motor unit spike trains and between EEG and motor unit spike trains. These analyses provide a systematic insight into the properties of the neural drive to the muscle in ET, and elucidate the causes of specific components of common input determining the pathological tremulous muscle activity.

Materials and methods

Subjects

We present results for nine patients (5 female, 4 male; age, mean ± SD: 71.0 ± 5.6 years, range 64–80 years) with a diagnosis of definite ET according to the criteria of the Tremor Investigation Group and the consensus of the Movement Disorder Society Group (Deuschl et al., 1998). All patients showed visible and persistent postural and kinetic tremor of the arms (unilateral or bilateral), and in some cases also at rest. No patient exhibited head or trunk tremor during the examination, or had a history of neurological diseases other than ET. None had features of parkinsonism (bradykinesia, rigidity) aside from isolated rest tremor. The mean disease duration was 22.7 ± 10.0 years (range 8–36 years). Tremor severity ranged from mild to severe, with a mean score in the most affected limb of 24.7 ± 7.0 (range 14–32), according to the Fahn-Tolosa-Marin scale. Four patients were taking anti-tremor drugs (propranolol 120 mg, 1 patient; propranolol sporadically, 1 patient; propranolol 60 mg and clonazepam 0.5 mg, 1 patient; propranolol 80 mg, 1 patient; all values indicate daily dosage), which in all cases were withheld for at least 12 h before the recordings. Patients were selected for enrolment by neurologists at two locations (3 at Hospital General Universitario, Valencia, Spain, and 6 at Hospital Universitario “12 de Octubre,” Madrid, Spain), starting 3 months before the experiments. They were identified from the database of patients from both hospitals after in-patient examination. No patient declined to participate in the study.

Ethical approval

The local ethical committees at Hospital 12 de Octubre, Madrid, Spain, and Universidad Politécnica de Valencia, Valencia, Spain, gave approval to the study, and warranted its accordance with the Declaration of Helsinki. All patients were informed beforehand, and signed a written informed consent to participate.

Recordings

Hand tremor at the most affected side (defined *in situ* after examination by a trained practitioner) was concurrently recorded with surface EMG and solid-state gyroscopes. Surface EMG was recorded with a 13 x 5 electrode grid with an inter-electrode distance of 8 mm (LISiN–OT Bioelettronica, Torino, Italy). The grid was placed over the extensors of the wrist, centered laterally above the extensor digitorum communis, and longitudinally above the muscle belly; a wrist bracelet soaked in water served as common reference. The signal was amplified (EMGUSB, OT Bioelettronica, Torino, Italy), band-pass filtered (10–750 Hz), and sampled at 2,048 Hz by a 12-bit A/D converter. Hand movement was measured with a pair of solid-state gyroscopes (Technaid S.L., Madrid, Spain) placed on the dorsum of the hand and the distal third of the forearm, by computing their difference (Rocon et al., 2006; Gallego et al., 2010). The raw gyroscope signals were sampled at 50 Hz by a 12-bit A/D converter, and low pass filtered (< 20 Hz). At the same time, EEG signals were recorded from 32 positions of the scalp, following the International 10-20 system (AFz, F3, F1, Fz, F2, F4, FC5, FC3, FC1, FCz, FC2, FC4, FC6, C5, C3, C1, Cz, C2, C4, C6, CP5, CP3, CP1, CPz, CP2, CP4, CP6, P3, P1, Pz, P2, and P4), with passive Au electrodes. The reference was set to the common potential of the two earlobes, and Az was used as ground. The signal was amplified (gUSBamp, g.Tec gmbh, Graz, Austria), band-pass (0.1–60 Hz) and notch (50 Hz) filtered, and sampled at 256 Hz by a 16 bit A/D converter. The recording systems were synchronized using a common clock signal generated by the computer acquiring the gyroscope data. The experiments were performed at Instituto de Biomecánica de Valencia, Valencia, Spain (patients 01–03), and Hospital 12 de Octubre, Madrid, Spain (patients 04–09). The data were stored and analyzed offline using Matlab (The Mathworks Inc., Natick MA, USA). Figures 1A to 1C show representative EEG, surface EMG and gyroscope signals.

[Figure 1 around here]

Procedure

The recordings were performed while patients were seated in a comfortable armchair, in a dimly illuminated room. Postural or rest tremor (depending on the patient) was elicited by asking the patients to keep the hands outstretched with palms down, parallel to the ground, while the forearms were fully supported on an armrest, or by asking them to relax with the hands hanging freely. The patients were instructed to stay relaxed and keep their gaze fixed on a wall at about 2 m distance, and those with mild tremor severity were asked to mentally count backwards during the recordings to enhance their tremor (Hellwig et al., 2001).

Patients performed a series of 4 min trials (between 1 and 3, depending on how they tolerated the setup, and on the quality of the recordings) of the task(s) that elicited their tremor. This ensured that we recorded at least one trial with tremor being present during most of the trial. For each patient, we present results for the trial during which tremor was most persistent.

Surface EMG Decomposition

Motor unit spike trains were identified from the multichannel surface EMG with the convolution kernel compensation (CKC) technique (Holobar and Zazula, 2007; Holobar et al., 2009), and manually verified by an experienced operator. The CKC technique has been validated with the decomposition of motor neuron activities in more than 15 muscles and 500 healthy subjects performing voluntary contractions (e.g. Holobar et al., 2009, 2010), and has been recently shown to work accurately also for EMG signals of tremor patients (Holobar et al., 2012). Specifically, the decomposition method has been shown to accurately decompose signals with paired and tripled discharges, i.e., firings with an ISI in the ~10–90 ms range, as observed in pathological tremor (Das Gupta, 1963; Dietz et al., 1974; Elek et al., 1991; Baker et al., 1992; Christakos et al., 2009). This technique is also the only one that was proved to be accurate for extremely high levels of motor unit synchronization (Holobar et al., 2012), as it may be expected in tremor.

Since the EMG decomposition accuracy was fundamental for assessing the properties of the neural drive to muscle and common synaptic inputs in ET patients, we defined two inclusion criteria for the identified single motor unit spike trains. First, given that the estimation of the characteristics of common inputs to motor neurons and the computation of corticospinal coherence typically require a sufficiently large number of epochs, we excluded those motor units that were not firing during more than 65 % of the trial. In addition, to ensure that only motor units whose spike trains were identified with great accuracy were considered in the analysis, we computed for each of them the signal-to-interference metric proposed in (Holobar et al., 2014). This metric assessed the quality of the decomposition by comparing the height of the spike trains identified to the baseline jitter of the CKC algorithm. A threshold of 28 dB was applied to this metric for the exclusion of motor units whose discharge patterns were not identified with high reliability (Holobar et al., 2014). Fig. 1 shows an example of decomposition of the surface EMG.

Data Processing and Analysis

This section presents the methodology employed to investigate motor unit synchronization, the characteristics of the common synaptic inputs to the motor neuron pool, and how the discharge pattern of individual and groups of motor neurons related to the tremor-related cortical activity. In some analyses several motor unit spike trains were pooled to build a so-called composite spike train (CST; Negro and Farina, 2011, 2012; Farina et al., 2013). The CST constitutes the best representation of the common synaptic input to motor neurons (Farina et al., 2013, 2014a), which is the neural drive to the muscle (Farina et al., 2014b), and is strongly correlated with muscle force (Negro et al., 2009). EEG channels were spatially filtered using the Hjorth transform (Hjorth, 1975) (16 electrodes: Fz, FC3, FC1, FCz, FC2, FC4, C3, C1, Cz, C2, C4, CP3, CP1, CPz, CP2, and CP4), and artefacts were carefully removed. Manual inspection, in combination with a threshold (defined as the mean ± 3 SD of a signal composed by 20 high-quality 1 -s epochs chosen from different parts of the trial) served to ensure that the resultant EEG signal did not contain significant artefacts.

Motor unit synchronization was estimated using a commonly employed technique (Nordstrom et al., 1992), which is based on the computation of cross-correlograms between pairs of motor unit spike trains (Kirkwood and Sears, 1978; Nordstrom et al., 1992). To this end, for each trial, we calculated the cross-correlation histogram and its correspondent cumulative sum (± 100 ms relative to the reference motor neuron discharge, in 1 ms bins; normalized by dividing each bin by the mean of the cross-correlation histogram) for all pairs of motor units. The position and duration of the synchronous peak in the cross-correlation histogram considered to be significant was calculated from the cumulative sum (Ellaway, 1978), by finding the first relative minimum moving backwards from the reference motor neuron discharge, and the first relative maximum moving forward (Dideriksen et al., 2009). We then considered this cross-correlation peak significant if the relative extrema of the cumulative sum function that identified it were above the mean of the baseline of the cross-correlogram by more than 3 SDs of the first 50 bins (Davey et al., 1986). Finally, the common input strength (CIS) index was computed for all pairs of motor neurons exhibiting significant synchronization, as the number of counts within the synchronous peak in excess of that expected by chance, divided by the time during which the motor units were active (Nordstrom et al., 1992). The last 2 min of the trial with stable motor unit firings were considered for these calculations, to enable comparison with the literature.

The frequency analysis of the common synaptic inputs to the motor neuron pool was performed by computing, for each trial, the mean coherence between all possible combinations of pairs of CSTs comprising the maximum possible number of different motor units (Negro and Farina, 2012). For example, if 7 motor units were identified from a muscle, we calculated the coherence function for each possible pair of CSTs comprising 4 and 3 different motor unit spike trains, and then averaged the coherence for all pairs. This has recently been shown to be the most effective means of characterizing the frequency content and strength of the common inputs to motor neurons (Negro and Farina, 2012). Furthermore, we investigated the relationship between motor unit synchronization as computed with the CIS and the common input strength as estimated from the coherence between pairs of CSTs by computing the CIS for the same data windows.

Finally, corticospinal coherence was computed to assess the cortical contribution to the neural drive to muscle, i.e. the CST. This allowed verifying the hypothesis that the central oscillations of ET are a common cortical projection to the motor neuron pool, and investigating their role as causative factors of the observed strength of common synaptic input. We calculated the corticospinal coherence between the 16 processed, artefact-free EEG channels and all the possible combinations of CSTs comprising between 1 and the total number of motor units identified during the trial. To test the hypothesis of common cortical projection to the motor neuron pool, we assessed, for the channel exhibiting the largest corticospinal coherence at the tremor frequency, how the coherence varied with the number of motor units considered: if the projection were common to the entire motor neuron pool, the coherence should increase monotonically, reaching a plateau, as more motor neurons were considered in the CST (Negro and Farina, 2011; Gallego et al., 2011).

The coherence functions between motor units and between motor units and EEG were calculated following the method proposed in Halliday et al. (1995). First, the CSTs and/or EEG signals were divided into epochs of 1-s duration, from which the individual power spectra and the cross-spectrum (1-s Hann window, 0.125 Hz resolution, achieved with zero-padding) were computed. Then, coherence was calculated as the ratio of the magnitude squared cross-spectrum to the product of their individual power spectra (e.g. Halliday et al., 1995; Hellwig et al., 2001). The confidence limit was obtained as proposed in Rosenberg et al. (1989).

Throughout the paper, results are given as mean ± SD. Statistical tests were considered significant if $P < 0.05$. Correlation between pairs of variables were investigated either using Pearson's or Spearman's correlation; the latter was employed when the data did not conform to normality (Lilliefor's test, $P < 0.05$). Differences in the strength of common input at different frequency bands were assessed using a Student's paired *t*-test. We tested whether motor unit synchronization as estimated with the CIS was significantly greater than for controls using a Wilcoxon signed rank test. To calculate the minimum number of motor neurons that most accurately transmitted the tremor-related cortical activity, we compared the magnitude of the coherence at the tremor frequency for the pooled data of all the patients with a Student's unpaired *t*-test. Pairs of corticospinal coherence estimates obtained for CSTs comprising n and $n + 1$ motor units were compared for increasing values of n until a non-significant difference was found.

Results

The total number of identified motor unit spike trains was 56 (6.2 ± 2.4 motor units per trial; see Table 1 for details). The average motor unit discharge rate over all patients had large variability, ranging from 9.0 ± 2.9 to 18.1 ± 3.9 pps (Table 1). There was no consistent relationship between motor unit firing rate and tremor frequency across patients (Fig. 2A). However, mean discharge rate was a poor indicator of motor unit properties since the ISI distributions varied among patients and included bimodal distributions. Therefore, we further analyzed the individual ISI histograms for each motor unit. The ISI histogram of the motor units discharges (Fig. 2B) followed either (1) a bimodal distribution (patients 01 to 04), with the first peak corresponding to paired or tripled discharges (average position of the peak, 34.6 ± 9.1 ms) and a second peak associated to the tremor frequency (average position, 190.5 ± 45.0 ms; see the representative examples in Fig. 1F, and Fig. 2B); or (2) a unimodal distribution (patients 05 to 09; average position of the peak, 67.3 ± 26.2 ms), with a peak not significantly correlated with the tremor frequency ($P = 0.100$, Spearman's correlation). The ISI histograms in Fig. 2 were built with all motor units together for each patient since all the units within a patient showed the same distribution of ISI. From Fig. 2A it is evident that there was no difference between the tremor frequency of the patients showing the two types of ISI distributions (range 4.8–6.1 Hz vs. 4.9–6.6 Hz, respectively). Finally, the relative proportion of paired and tripled discharges (range 37.43–68.15 % for those patients with a bimodal ISI histogram) varied considerably among motor units and patients, as reported for patients with Parkinson's disease (Dietz et al., 1974; Christakos et al., 2009).

[Table 1 and Figure 2 around here]

Motor unit synchronization

The analysis of cross-histograms of motor unit spike trains pairs indicated that the activities of 132 out of 169 motor unit pairs (78.1 %) were significantly synchronized. The average CIS over all motor units of all patients was 1.44 ± 1.44 pps (see values per patient in Table 1), an average value significantly greater ($P < 0.001$, Wilcoxon signed rank test) than that reported for healthy subjects for the same muscle group during voluntary contractions (mean value ≤ 0.7 pps; Keen and Fuglevand, 2004; Schmied et al., 1993). The CIS value was not associated to the tremor frequency ($P = 0.472$, Pearson's correlation).

Sources of Common Inputs to Motor Neurons

Fig. 3 shows the coherence analysis between populations of motor units for each patient. In all cases there were two large peaks in the coherence spectrum, which indicated the presence of two main sources of common input to the motor neuron pool: one at low frequency (< 2–3 Hz), presumably related to the voluntary common drive to muscle (De Luca and Erim, 1994; Negro and Farina, 2009, 2012), and a second peak at the tremor frequency (mean frequency 5.5 ± 0.9 Hz, indicated with black arrows in Fig. 3). This suggests that, in addition to the common drive that reflected the neural control of voluntary contractions (8 out of 9 patients were holding their hands outstretched), the motor neuron pool received common input at the tremor frequency. The extent to which both common synaptic inputs were shared across the motor neurons (i.e., coherence values at the two frequencies) were independent of each other ($P = 0.795$, Pearson's correlation), being the coherence at the tremor frequency significantly greater ($P = 0.002$, Student's paired *t*-test). These common inputs may not only reflect the descending drive to muscle, but also the contribution of spinal afferents (Farina et al., 2010; Dartnall et al., 2008). The coherence spectra of patients 01, 02 and 08 also exhibited clear peaks at frequencies that were harmonics of that of the tremor (Fig. 3). Because two of these patients (01 and 02) had a bimodal ISI histogram contrary to 08 (Fig. 2), these coherence peaks were not associated to the type of ISI distribution.

Direct examination of the motor unit spike trains explains the high coherence at the tremor frequency. Fig. 4 shows the filtered motor unit spike trains (band-pass, 3–10 Hz, zero phase), which in the tremor band are oscillations at the same frequency and phase as the tremor oscillations. The similarity of these oscillations among motor units indicates the common nature of the generating input.

[Figure 3 and Figure 4 around here]

Finally, the mean coherence value between CSTs at the tremor frequency was significantly correlated with the mean CIS (calculated using the same data windows; see Fig. 3) across patients ($P = 0.005$, $r = 0.840$, Pearson's correlation).

Corticospinal Coupling

The average number of 1-s epochs per subject not influenced by EEG artefacts, and with stable discharges of the identified motor neurons, was 97.4 ± 50.6 (range 36-182). These were the data used in the calculations of corticospinal coupling.

Fig. 5 displays an example of corticospinal coherence as estimated from the motor unit activities and the processed EEG signal recorded at the contralateral sensorimotor cortex (where the largest coherence was found, as expected). The plots of coherence correspond to the functions obtained when varying the number of motor unit spike trains used for the calculation (from 1 to 11, in this example). The coherence peak at the tremor frequency (~4.75 Hz, indicated with the red arrow in Fig. 5A) was above confidence level for any number of motor units, even when using only one unit, indicating a strong tremor-related cortical projection. Moreover, the magnitude of the corticospinal coherence at the tremor frequency increased monotonically with the number of motor neurons considered, until a plateau was reached when ~5 motor neurons were included in the CST (Fig. 5B). Considering more than five motor units for the estimate increased negligibly the amount of coherence (for example, the increase when considering 6 motor units was 0.5 % with respect to 5, and when considering 11, it was 1.5 % with respect to 5). The estimation of corticospinal coherence was relatively invariant to which motor units were chosen to build the CST, as shown by the small SD of the values in Fig. 5B. These observations verify the hypothesis that the descending tremor-related cortical activity was common to the entire motor neuron pool (Negro and Farina, 2011; Gallego et al., 2011). The coherence spectra also showed a significant peak at the beta band (indicated with a blue arrow in Fig. 5A), which is related to voluntary descending commands (e.g., Conway et al., 1995; Negro and Farina, 2011). The coherence in this band also increased monotonically as more motor units were considered, but the trend was slower and the values had greater SD than for the coherence at the tremor band (Fig. 5B). Therefore, for this patient differences existed in the manner in which both descending drives were projected to the output of the motor neuron pool. As expected, the frequency of the hand oscillations corresponded to the tremor frequency peak of the corticospinal coherence (indicated with a red arrow in Fig. 5A and Fig. 5C).

[Figure 5 around here]

Similar results were obtained for all the patients analyzed (Table 1). In all cases, the corticospinal coherence function showed a significant peak at the tremor frequency and, in 8 patients, another peak in the beta band. Significant coherence at the beta band was found even in the patient who performed the rest task (patient 02, see Table 1), which implies that also in this case there was a certain amount of voluntary descending command. The only patient who did not show significant corticospinal coherence in the beta band was the one with the greatest number of signal epochs excluded due to artefacts. The relatively small number of epochs (49) used for the computation of coherence may have been not sufficient to identify a significant coherence level at high frequencies. Finally, it is worth observing that, although always above the confidence level, the corticospinal coherence values at the tremor frequency were relatively small (Fig. 5 and Table 1).

As observed for patient 03 (Fig. 5B), in all the patients the corticospinal coherence at the tremor frequency increased monotonically as more motor units were included in the CST, and concurrently the variability of the estimate decreased (Fig. 6A). Moreover, in all patients, the coherence values tended to a maximum when using a relatively small number of units (Fig. 6A). The statistical analysis of the pooled data of all patients indicated that 5 motor units ($P < 0.05$, Student's unpaired *t*-test) resulted in an accurate transmission of the corticospinal input, i.e. the increase in corticospinal coherence was negligible after using 5 motor units for the estimate. As mentioned above, this indicates that tremor was a common cortical projection to the motor neuron pool (Negro and Farina, 2011). Interestingly, for seven patients (all except patients 02 and 08) the estimation of corticospinal coherence with only 1 motor unit showed a peak at the tremor frequency above the confidence level, as for the representative case of Fig. 5. This indicated that in most cases the descending cortical tremor input was sufficiently strong that it could even be observed in the output of a single motor neuron.

The magnitude of the coherence in the beta band increased monotonically with the number of units for all patients, as for the tremor frequency, but did not reach a constant value using the maximum number of detected units.

[Figure 6 around here]

Finally, we found no significant relation between the magnitude of the corticospinal coherence at the tremor frequency and the corresponding peak in the coherence between CSTs ($P = 0.445$, Pearson's correlation).

Discussion

We have systematically investigated the characteristics of the motor unit spike trains in ET patients, and the sources of common synaptic input that the motor neurons receive. This analysis was possible due to a recently developed method of decomposition of multichannel surface EMG recordings (Holobar et al., 2012) that circumvents the methodological limitations of traditional approaches using intramuscular electrodes (Merletti and Farina, 2009). This study demonstrates, for the first time, that the motor units in ET patients exhibit greater degree of synchronization than in healthy individuals, which implies the existence of strong common synaptic inputs to the motor neuron pool. The high level of common input to motor neurons was confirmed by the analysis of coherence between CSTs, which showed that the increase in synchronization occurs mainly due to a common input at the tremor frequency. Corticospinal coupling, studied between EEG and CSTs, indicated that the tremor-related cortical activity is a common projection to the motor neuron pool.

Despite the relative similarity in the mechanical manifestation of tremor among patients, the underlying motor unit discharges had different statistical distributions (see Fig. 2). Nonetheless, the properties of the common input were consistent across patients as revealed by the analysis of coherence between CSTs that showed two main inputs for all patients. Since the degree of motor unit synchronization was correlated to the coherence value at the tremor frequency, synchronization among motor units was increased by the common synaptic input at the tremor frequency (Sears and Stagg, 1976; Kirkwood and Sears, 1978; Nordstrom et al., 1992). Indeed, motor unit synchronization provides an estimate of the global strength of synaptic input for the entire frequency bandwidth whereas coherence shows synchronization for each frequency (Negro and Farina, 2012). The data presented provide the first experimental proof of high synchronization levels among motor units in ET patients, and show that high synchronization occurs specifically with an oscillation at the tremor frequency, thus causing rhythmic entrainment that contributes to the generation of tremor. This association has been previously hypothesized (e.g., Elek et al., 1991; McAuley and Marsden, 2000; Elble and Deuschl, 2009) but never directly proven. Based on evidence that motor unit synchronization does not differ between young and old adults (Kamen and Roy, 2000; Semmler et al., 2000), we conclude that this greater than normal synchronization was caused by the tremor input to motor neurons, and was not an effect of age.

Previous studies reported that the cortical oscillations causing ET are projected to tremulous muscles through the corticospinal tract, based on the observation of significant coherence at the tremor frequency between EEG and EMG recordings (Hellwig et al., 2001, 2003; Raethjen et al., 2007; Muthuraman et al., 2012). We re-analyzed these observations by computing the coherence between EEG and motor unit spike trains. With our analysis at the single motor unit level, we also found significant corticospinal coherence between the contralateral sensorimotor cortex and motor unit cumulative spike train (CST; see Table 1), confirming the studies based on the interference EMG. Despite the agreement in conclusions based on EEG-EMG coherence and our EEG-motor unit coherence data, we showed the association between EEG and motor neuron output directly, which is a stronger evidence of a direct influence of the corticospinal tract in tremor generation (Negro and Farina, 2011). Furthermore, we also studied the behavior of coherence with EEG when the number of motor unit spike trains considered was progressively increased. This analysis showed that as more motor unit spike trains were analyzed, the coherence at the tremor frequency increased monotonically, up to a constant value reached for ~5 motor units, and the variability of coherence estimates decreased (Fig. 6A). These observations indicate not only the presence of corticomuscular coupling but also that the central oscillations causing ET are a common projection to the entire motor neuron pool (Negro and Farina, 2011; Gallego et al., 2011). On the basis of the present results, it is unlikely that intermittent nonlinear corticomuscular interaction participates in the transmission of the central oscillations that cause ET, as proposed by Raethjen et al. (2007).

Concurrently with the presence of significant corticospinal coupling at the tremor frequency, we also observed significant coherence between the EEG and motor unit spike trains in the beta band. This is assumed to represent the voluntary drive sent to motor neurons by the corticospinal tract (e.g. Conway et al., 1995; Negro and Farina, 2011). Therefore, in ET patients the motor neuron pool concurrently samples two strong common inputs with different frequency content, which likely facilitates the occurrence of tremor during the performance of voluntary movements (e.g. Deuschl et al., 2000; Benito-León and Louis, 2006). Notably, both common synaptic inputs are also observed directly from the analysis of coherence between CSTs at the spinal level (see Fig. 3).

Since the strength corticospinal coupling at the tremor frequency was uncorrelated with the magnitude of the coherence between CSTs (that represents the net common synaptic input) at the same frequency, it is unlikely that the cortical input was the only source of common input to motor neurons at the tremor frequency. Accordingly, the corticospinal coherence values were very low, as in previous work (Raethjen et al., 2007), which indicates the presence of additional sources of common input at the tremor frequency that may decrease the correlation with the common cortical input (Negro and Farina, 2011b). We therefore hypothesize that the afferent component, which is projected to the entire motor neuron pool by Ia fibres (Mendell and Henneman, 1971), or additional supraspinal descending drives, provide a substantial contribution to the common input received by motor neurons at the tremor frequency. The potential role of the afferent input, in particular, is in agreement with evidence showing that the modification of the mechanical properties of the tremulous limb alters the tremor in ET (e.g., Héroux et al., 2009; Elble et al., 1987). Moreover, the observation that in some cases there were significant peaks at the first tremor frequency harmonic in the coherence between CSTs (Fig. 3) while these peaks were never observed in the EEG-CST coherence (see example in Fig. 5), indicates that they were likely generated by common projections of afferent pathways due to their resonant behavior. The hypothesis that muscle spindles contribute significantly to the generation of the tremor in ET could be further investigated by experiments manipulating the level of afferent activity. For example, reduction of Ia activity by means of localized ischemia (Allum and Mauritz, 1984; Sinkjaer and Hayashi, 1989) or by the restriction of limb movement (isometric conditions) could be applied and the effect on the neural drive to the muscle and the corticospinal coherence could be assessed.

In conclusion, this study systematically analyses for the first time the neural drive to muscle in ET patients using a novel non-invasive approach that offers a unique view into the output of the spinal cord circuitries in vivo. We demonstrated that motor units in ET are highly synchronized because of the presence of strong common synaptic input to motor neurons at the tremor frequency. This common input is partly corticospinal, as shown by the analysis of coherence between EEG and motor unit spike trains. However, it is weakly associated with the net common input at the tremor frequency (coherence between CSTs), which indicates a contribution of common input from spinal or secondary supraspinal sources. These data are the first that provide a complete description of the characteristics of motor unit spike trains in ET.

Author Contributions:

J.A.G., J.L.D., A.H., E.R., and D.F. conception and design of research; J.A.G., A.H., J.I., E.R. performed experiments; J.A.G., J.L.D., A.H., J.I., analyzed data; J.A.G., J.L.D., A.H., J.I., E.R., E.D.L., and D.F. interpreted results of experiments; J.A.G., prepared figures; J.A.G., J.L.D., and D.F., drafted the manuscript; J.A.G., J.L.D., A.H., J.I., J.L.P., E.D.L., E.R., and D.F., edited and revised the manuscript; J.A.G., J.L.D., A.H., J.I., J.L.P., E.D.L., E.R., and D.F., approved final version of manuscript.

Acknowledgments

The authors gratefully thank Dr. Juan Manuel Belda-Lois (Instituto de Biomecánica de Valencia, Valencia, Spain) and Dr. Ascensión Castillo (Hospital General de Valencia, Valencia, Spain) for their help with the experiments at Valencia, and Mr. Juan Pablo Romero, Dr. Ignacio Javier Posada-Rodríguez, Dr. Félix Bermejo-Pareja, and Dr. Julián Benito-León (University Hospital "12 de Octubre," Madrid, Spain) for their help with the experiments at Madrid.

Grants

This work was funded by the EU Commission [grant number EU-FP7-2011-287739 (NeuroTREMOR)].

Competing Interests

The authors declare no competing interests.

References

Allum J, Mauritz K. Compensation for intrinsic muscle stiffness by short-latency reflexes in human triceps surae muscles. *J Neurophysiol* 52: 797-818, 1984.

Baker JR, Davey NJ, Ellaway PH, Friedland CL. Short-term synchrony of motor unit discharge during weak isometric contraction in Parkinson's disease. *Brain* 115: 137–54, 1992.

Benito-León J, Louis ED. Essential tremor: emerging views of a common disorder. *Nat Clin Pract Neurol* 2: 666–78, 2006.

Boonstra TW, Roerdink M, Daffertshofer A, van Vugt B, van Werven G, Beek PJ. Low-alcohol doses reduce common 10- to 15-Hz input to bilateral leg muscles during quiet standing. *J Neurophysiol* 100: 2158–64, 2008.

Christakos CN, Erimaki S, Anagnostou E & Anastasopoulos D. Tremor-related motor unit firing in Parkinson's disease: implications for tremor genesis. *J Physiol* 587: 4811–27, 2009.

Conway BA, Halliday DM, Farmer SF, Shahani U, Maas P, Weir AI, Rosenberg JR. Synchronization between motor cortex and spinal motoneuronal pool during the performance of a maintained motor task in man. *J Physiol* 489: 917–24, 1995.

Dartnall TJ, Nordstrom MA, Semmler JG. Motor unit synchronization is increased in biceps brachii after exercise-induced damage to elbow flexor muscles. *J Neurophysiol* 99: 1008–19, 2008.

Das Gupta A. Paired response of motor units during voluntary contraction in Parkinsonism. *J Neurol Neurosurg Psychiatry* 26: 265–8, 1963.

Davey N, Ellaway P, Stein R. Statistical limits for detecting change in the cumulative sum derivative of the peristimulus time histogram. *J Neurosci Methods* 17: 153–66, 1986.

De Luca CJ, Erim Z. Common drive of motor units in regulation of muscle force. *Trends Neurosci* 17: 299–305, 1994.

Deuschl G, Bain P, Brin M. Consensus statement of the Movement Disorder Society on Tremor. Ad Hoc Scientific Committee. *Mov Disord* 13: *Suppl* 3, 2–23, 1998.

Deuschl G, Wenzelburger R, Löffler K, Raethjen J, Stolze H. Essential tremor and cerebellar dysfunction clinical and kinematic analysis of intention tremor. *Brain* 123: 1568–80, 2000.

Deuschl G, Raethjen J, Lindemann M, Krack P. The pathophysiology of tremor. *Muscle Nerve* 24: 716–35, 2001.

Dideriksen JL, Falla D, Baekgaard M, Mogensen ML, Steimle KL, Farina D. Comparison between the degree of motor unit short-term synchronization and recurrence quantification analysis of the surface EMG in two human muscles. *Clin Neurophysiol* 120: 2086–92, 2009.

Dietz V, Hillesheimer W, Freund H. Correlation between tremor, voluntary contraction, and firing pattern of motor units in Parkinson's disease. *J Neurol Neurosurg Psychiatry* 37: 927–37, 1974.

Elble RJ, Deuschl G. An update on essential tremor. *Curr Neurol Neurosci Rep* 9: 273–7, 2009.

Elble RJ, Higgins C, Moody CJ. Stretch reflex oscillations and essential tremor. *J Neurol Neurosurg Psychiatry* 50: 691–8, 1987.

Elek JM, Dengler R, Konstanzer A, Hesse S, Wolf W. Mechanical implications of paired motor unit discharges in pathological and voluntary tremor. *Electroencephalogr Clin Neurophysiol* 81: 279–83, 1991.

Ellaway P. Cumulative sum technique and its application to the analysis of peristimulus time histograms. *Electroencephalogr Clin Neurophysiol* 45: 302–4, 1978.

Farina D, Holobar A, Merletti R, Enoka RM. Decoding the neural drive to muscles from the surface electromyogram. *Clin Neurophysiol* 121: 1616–23, 2010.

Farina D, Negro F, Jiang N. Identification of common synaptic input to motor neurons from the rectified electromyogram. *J Physiol* 591: 2403–18, 2013.

Farina D, Negro F, Jiang N. Reply from Dario Farina, Francesco Negro and Ning Jiang. *J Physiol* 592: 251–2, 2014a.

Farina D, Negro F, Dideriksen JL. The effective neural drive to muscles is the common synaptic input to motor neurons. *J Physiol* doi: 10.1113/jphysiol.2014.273581, 2014b.

Farmer SF, Swash M, Ingram DA, Stephens JA. Changes in motor unit synchronization following central nervous lesions in man. *J Physiol* 463: 83–105, 1993.

Gallego JA, Rocon E, Roa JO, Moreno JC, Pons JL. Real-time estimation of pathological tremor parameters from gyroscope data. *Sensors (Basel)* 10: 2129–49, 2010.

Gallego JA, Dideriksen JL, Farina D, Rocon E, Holobar A, Pons JL. A modelling study on the transmission of the central oscillator in tremor by a motor neuron pool. *Conf Proc IEEE Eng Med Biol Soc* 2037–40, 2011.

Halliday DM, Rosenberg JR, Amjad AM, Breeze P, Conway BA, Farmer SF. A framework for the analysis of mixed time series/point process data–theory and application to the study of physiological tremor, single motor unit discharges and electromyograms. *Prog Byophys Mol Biol* 64: 237–78, 1995.

Heckman CJ, Enoka RM. Motor unit. *Compr Physiol* 2(4), 2629–82, 2012.

Hellwig B, Häußler S, Schelter B, Lauk M, Guschlbauer B, Timmer J, Lücking CH. Tremor-correlated cortical activity in essential tremor. *Lancet* 357: 519–523, 2001.

Hellwig B, Schelter B, Guschlbauer B, Timmer J, Lücking C. Dynamic synchronisation of central oscillators in essential tremor. *Clin Neurophysiol* 114: 1462–7, 2003.

Héroux ME, Pari G, Norman KE. The effect of inertial loading on wrist postural tremor in essential tremor. *Clin Neurophysiol* 120: 1020–9, 2009.

Hjorth B. An on-line transformation of EEG scalp potentials into orthogonal source derivations. *Electroencephalogr Clin Neurophysiol* 39: 526–30, 1975.

Holobar A, Zazula D. Multichannel Blind Source Separation Using Convolution Kernel Compensation. *IEEE Trans Signal Process* 55: 4487–96, 2007.

Holobar A, Farina D, Gazzoni M, Merletti R, Zazula D. Estimating motor unit discharge patterns from high-density surface electromyogram. *Clin Neurophysiol* 120: 551–62, 2009.

Holobar A, Minetto MA, Botter A, Negro F, Farina D. Experimental analysis of accuracy in the identification of motor unit spike trains from high-density surface EMG. *IEEE Trans Neural Syst Rehabil Eng* 18: 221–9, 2010.

Holobar A, Glaser V, Gallego JA, Dideriksen JL, Farina D. Non-invasive characterization of motor unit behavior in pathological tremor. *J Neural Eng* 9: 056011, 2012.

Holobar A, Minetto MA, Farina D. Accurate identification of motor unit discharge patterns from high-density surface EMG and validation with a novel signal-based performance metric. *J Neural Eng* 11: 016008, 2014.

Kamen G, Roy A. Motor unit synchronization in young and elderly adults. *Eur J Appl Physiol* 81: 403–410, 2000.

Keen DA, Fuglevand AJ. Common input to motor neurons innervating the same and different compartments of the human extensor digitorum muscle. *J Neurophysiol* 91: 57–62, 2004.

Kirkwood P, Sears TA. The synaptic connections to intercostal motoneurones as revealed by the average common excitation potential. *J Physiol* 275: 103–134, 1978.

Kudina LP, Andreeva RE. Motoneuron double discharges: only one or two different entities? *Front Cell Neurosci* 7: 75, 2013.

Louis ED, Babij R, Cortés E, Vonsattel JP, Faust PL. The inferior olivary nucleus: a postmortem study of essential tremor cases versus controls. *Mov Disord* 28: 779–86, 2013.

McAuley JH, Marsden CD. Physiological and pathological tremors and rhythmic central motor control. *Brain* 123: 1545–67, 2000.

Mendell LM, Henneman E. Terminals of single Ia fibers: location, density, and distribution within a pool of 300 homonymous motoneurons. *J Neurophysiol* 34: 171–187, 1971.

Merletti R, Farina D. Analysis of intramuscular electromyogram signals. *Philos Trans A Math Phys Eng Sci* 367: 357–68, 2009.

Muthuraman M, Heute U, Arning K, Anwar AR, Elble R, Deuschl G, Raethjen J. Oscillating central motor networks in pathological tremors and voluntary movements. What makes the difference? *Neuroimage* 60: 1331–1339, 2012.

Negro F, Farina D. Linear transmission of cortical oscillations to the neural drive to muscles is mediated by common projections to populations of motoneurons in humans. *J Physiol* 589: 629–37, 2011.

Negro F, Farina D. Decorrelation of cortical inputs and motoneuron pool. *J Neurophysiol* 106: 2688–97, 2011b.

Negro F, Farina D. Factors influencing the estimates of correlation between motor unit activities in humans. *PLoS One* 7: e44894, 2012.

Negro F, Holobar A, Farina D. Fluctuations in isometric muscle force can be described by one linear projection of low-frequency components of motor unit discharge rates. *J Physiol* 587: 5925–38, 2009.

Nordstrom M, Fuglevand AJ, Enoka RM. Estimating the strength of common input to human motoneurons from the cross-correlogram. *J Physiol* 453: 547–74, 1992.

Raethjen J, Govindan RB, Kopper F, Muthuraman, Deuschl G. Cortical involvement in the generation of essential tremor. *J Neurophysiol* 97: 3219–28, 2007.

Rocon E, Andrade AO, Pons JL, Kyberd P, Nasuto SJ. Empirical mode decomposition: a novel technique for the study of tremor time series. *Med Biol Eng Comput* 44: 569–82, 2006.

Schmied A, Ivarsson C, Fetz EE. Short-term synchronization of motor units in human extensor digitorum comunis muscle: relation to contractile properties and voluntary control. *Exp Brain Res* 97: 159–72, 1993.

Sears TA, Stagg D. Short-term synchronization of intercostal motoneurone activity. *J Physiol* 263: 357–81, 1976.

Semmler JG, Steege JW, Kornatz KW, Enoka RM. Motor-unit synchronization is not responsible for larger motor-unit forces in old adults. *J Neurophysiol* 84: 358–366, 2000.

Sinkjaer T, Hayashi R. Regulation of wrist stiffness by the stretch reflex. *J Biomech* 22: 1133–40, 1989.

Figure 1 Example of EEG, surface EMG, and gyroscope signals recorded, and of a few motor units identified through the decomposition of the multichannel surface EMG. The data corresponds to patient 03. **(A)** shows recordings from 3 EEG channels, **(B)** displays signals from all the channels of the fourth column of the surface EMG electrode array (rows 1 to 12), and **(C)** represents hand tremor as recorded with a pair of gyroscopes. The rest of the plots are related to motor unit discharges: **(D)** shows the shape of the motor unit action potential of one of the motor neurons identified, for all the channels of the fourth and fifth columns of the electrode array (rows 1 to 12), **(E)** displays the spike trains discharged by 5 of the motor units identified for this patient, and **(F)** depicts the ISI histogram of two of these motor neurons, exhibiting a clear bimodal pattern caused by the occurrence of paired (or tripled) discharges and the subsequent firings to complete a tremor burst.

Figure 2 Relationship between the statistical properties of the discharges of the detected motor units and the frequency of tremor. (**A**) Mean + SD (circles and whiskers respectively) of the average motor unit discharge rate of all of the motor units detected for each patient. The number besides each circle represents the patient code. SDs are scaled by 1/2 to facilitate visualization. (**B**) Cumulative ISI histograms for the motor units detected for each patient. The number again represents the patient code. In each histogram *n* indicates the number of motor units. The mean discharge rate was computed excluding firings with ISI < 10 ms or > 3·median(ISI). DR = discharge rate.

Figure 3 Estimation of common synaptic inputs to the motor neurons identified, for all the patients. The plots show the coherence spectra for all possible pairs of CSTs comprising each the largest possible amount of motor unit spike trains (in grey), with their mean (solid black trace) ± SD (dashed black trace). Each panel represents a single patient. The frequency bands that correspond to the common voluntary drive and the common input at the tremor frequency are shaded in blue and red respectively. The mean ± SD CIS for the same data window that were employed to compute the coherence between pairs of CSTs is displayed on top of each plot.

Figure 4 Examples of motor unit spike trains for 3 patients. The figure shows, for each of them, the firings of 5 motor units randomly chosen among those identified, and their filtered version (band-pass, 3–10 Hz, zero phase) at the top and the bottom of each panel (displayed in the same color), respectively. Both are compared to the hand motion (light grey traces in the background) to emphasize how the motor units encode the tremor. Paired discharges are marked with a dot on top of the discharge. The plot illustrates the observed large motor unit synchronization, and how motor unit firing patterns sometimes fluctuate (see patient 05).

Figure 5 Example of coherence between EEG signals recorded at the contralateral sensorimotor cortex (FC4, given that we recorded the left hand) and the CSTs. The data are from patient 03. (**A**) Average coherence for all possible CSTs comprising from 1 to 11 motor neurons (black, solid lines). These coherence spectra always exhibited a significant peak at tremor frequency (black arrow), whose height increased monotonically with the number of motor units considered. Coherence at the beta band (gray arrow), corresponding to the voluntary drive to muscle, which became significant when 7 motor units were included in the CST. The confidence level ($P < 0.05$) is represented as a dashed black line. (**B**) Mean ± SD (the circle and the length of the whiskers respectively) of the coherence at tremor frequency (in black; it corresponds to the peak indicated with the black arrow in A) and the beta band (in gray; it corresponds to the peak indicated with the gray arrow in A) as function of the number of motor units in the CST. (**C**) Amplitude spectrum of the hand tremor as recorded with the solid-state gyroscopes, showing a clear peak at tremor frequency (red arrow), which appeared very close to that observed in the coherence plots depicted in (A). (**D**) Hand oscillations during a portion of the trial.

Figure 6 Estimation of corticospinal coherence at the tremor frequency (left) and the beta band (right) as function of the number of motor units considered, for all patients. The circles and their whiskers represent the mean ± SD of the coherence peak at the selected frequency, obtained for all the possible combinations of motor units to form a CST. Results are shown as function of the number of motor units included in the calculations, and each patient is represented in a different color. Patients are codified as follows: data from patient 01 are displayed in black, from patient 02 in red, from patient 03 in blue, from patient 04 in green, from patient 05 in cyan, from patient 06 in yellow, from patient 07 in magenta, from patient 08 in brown, and from patient 09 in orange. A series of grand means are also displayed (thick black lines) to represent the general trend of the data: for all the patients (diamonds), for all the patients with 5 or more motor units detected (circles), for all the patients with 6 or more motor units detected (squares), for all patients with 7 or more motor units detected (crosses), and for all patients with 9 or more motor units detected (triangles).

Patient	01	02	03	04	05	06	07	08	09
Type of tremor	PO	RE	PO	PO	PO	PO	PO	PO	PO
Num. MUs.	5	5	11	4	5	4	9	7	6
Avg. disch. rate (pps)	10.0 ± 2.6	12. 7 ± 4.9	18.1 ± 3.9	13.1 ± 2.4	17.7 ± 1.4	16.3 ± 1.1	16.2 ± 3.4	9.00 ± 2.9	14.70 ± 2.2
CIS [2 min] (pps)	1.45 ± 0.22	0.98 ± 1.47	2.32 ± 1.96	0.95 ± 0.76	1.61 ± 0.48	1.63 ± 1.00	1.46 ± 1.27	0.36 ± 0.53	0.96 ± 0.92
EEG channel	C3	C1	FC4	FC3	CP3	CP4	FC2	CP3	CP2
Coh. tremor	0.029	0.027	0.046	0.090	0.060	0.045	0.156	0.083	0.119
Freq. tremor (Hz)	5.5	4.9	4.7	6.1	5.7	4.9	5.9	6.6	6.2
Coh. Beta	0.034	0.025	0.031	0.063	0.054	0.034	n.s.	0.064	0.185
Freq. beta (Hz)	27.3	12.4	29.3	12.4	26.9	15.3	n.s.	20.1	17.6

[Table 1]

Table 1. Summary of motor neuron synchronization and corticospinal coherence. The table shows, for each patient, the type of tremor elicited (postural, PO or rest, RE), the number of motor units identified through the decomposition of the surface EMG, the grand mean (± SD) of their discharge rate, the degree of motor unit synchronization according to the CIS (the last 2 variables were computed in 2 min windows), the EEG channel that exhibited the largest coherence at the tremor frequency, and the magnitude and frequency at which the coherence peaks at the tremor frequency and the beta band were found. All coherence values reported were statistically significant ($P < 0.05$), except where noted otherwise (n.s.).

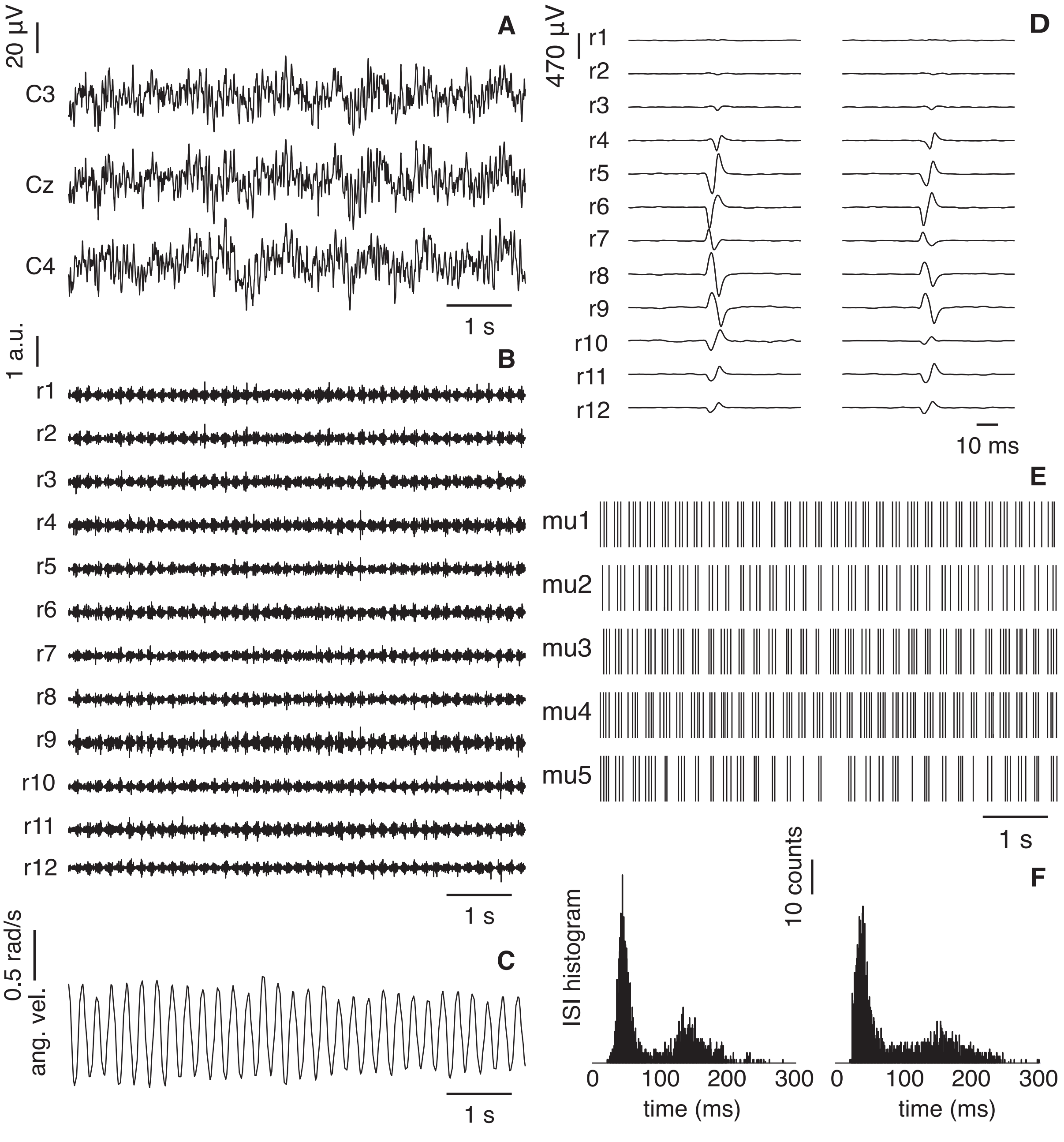
A
20 µV
C3
Cz
C4
1 s
B
1 a.u.
r1
r2
r3
r4
r5
r6
r7
r8
r9
r10
r11
r12
1 s
C
0.5 rad/s
ang. vel.
1 s
D
470 µV
r1
r2
r3
r4
r5
r6
r7
r8
r9
r10
r11
r12
10 ms
E
mu1
mu2
mu3
mu4
mu5
1 s
F
10 counts
ISI histogram
0
100
200
300
time (ms)
0
100
200
300
time (ms)

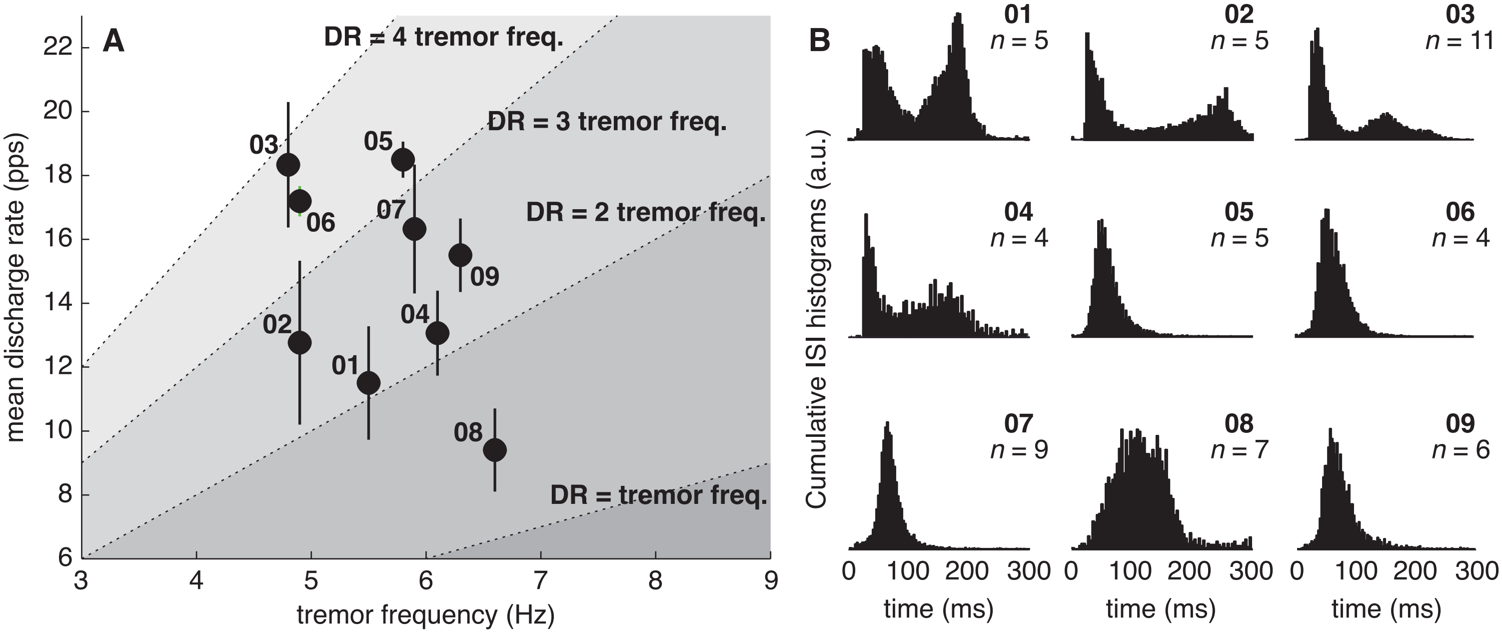
A
DR = 4 tremor freq.
DR = 3 tremor freq.
DR = 2 tremor freq.
DR = tremor freq.
mean discharge rate (pps)
tremor frequency (Hz)
22
20
18
16
14
12
10
8
6
3
4
5
6
7
8
9
03
05
06
07
09
02
04
01
08
B
Cumulative ISI histograms (a.u.)
01
n = 5
02
n = 5
03
n = 11
04
n = 4
05
n = 5
06
n = 4
07
n = 9
08
n = 7
09
n = 6
0
100
200
300
time (ms)
time (ms)
time (ms)

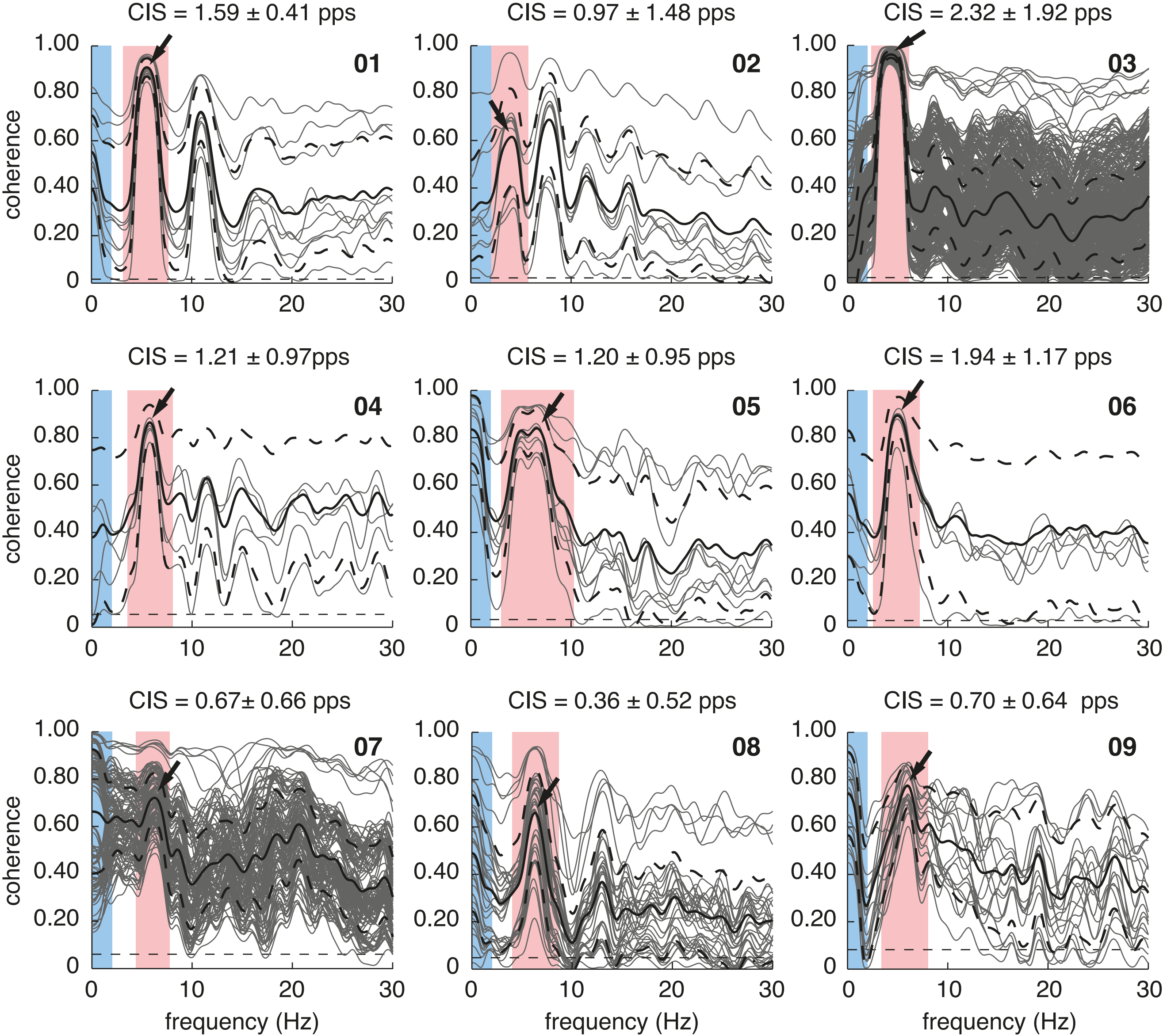

CIS = 1.59 ± 0.41 pps

CIS = 0.97 ± 1.48 pps

CIS = 2.32 ± 1.92 pps

CIS = 1.21 ± 0.97pps

CIS = 1.20 ± 0.95 pps

CIS = 1.94 ± 1.17 pps

CIS = 0.67± 0.66 pps

CIS = 0.36 ± 0.52 pps

CIS = 0.70 ± 0.64 pps

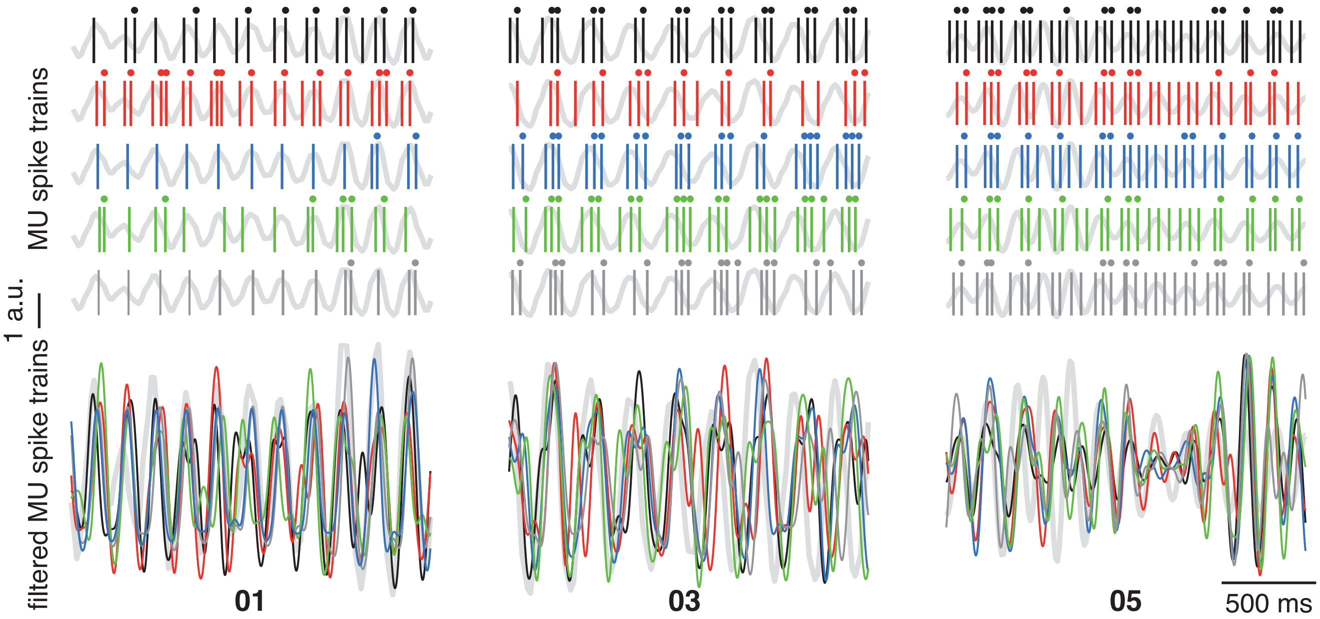
MU spike trains
1 a.u.
filtered MU spike trains
01
03
05
500 ms

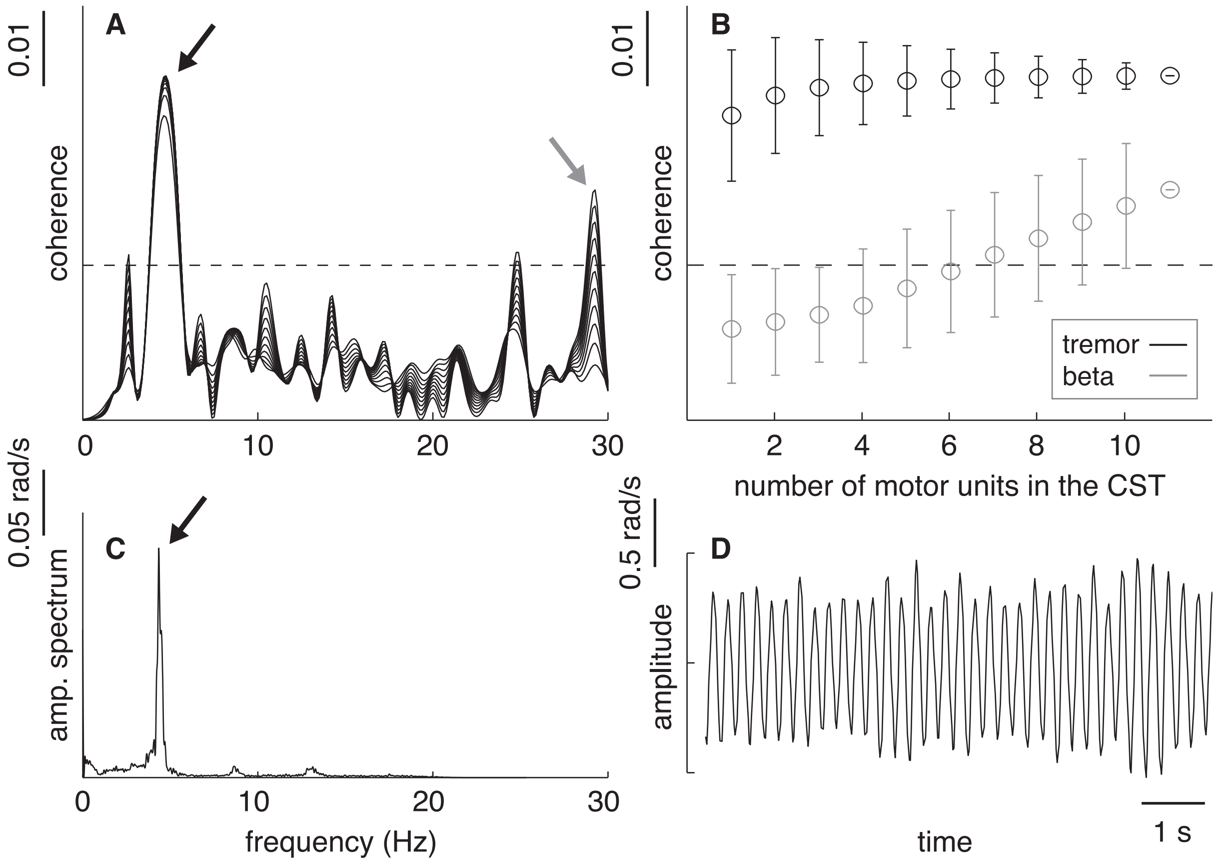
A
0.01
coherence
0
10
20
30
B
0.01
coherence
tremor
beta
2
4
6
8
10
number of motor units in the CST
C
0.05 rad/s
amp. spectrum
0
10
20
30
frequency (Hz)
D
0.5 rad/s
amplitude
time
1 s

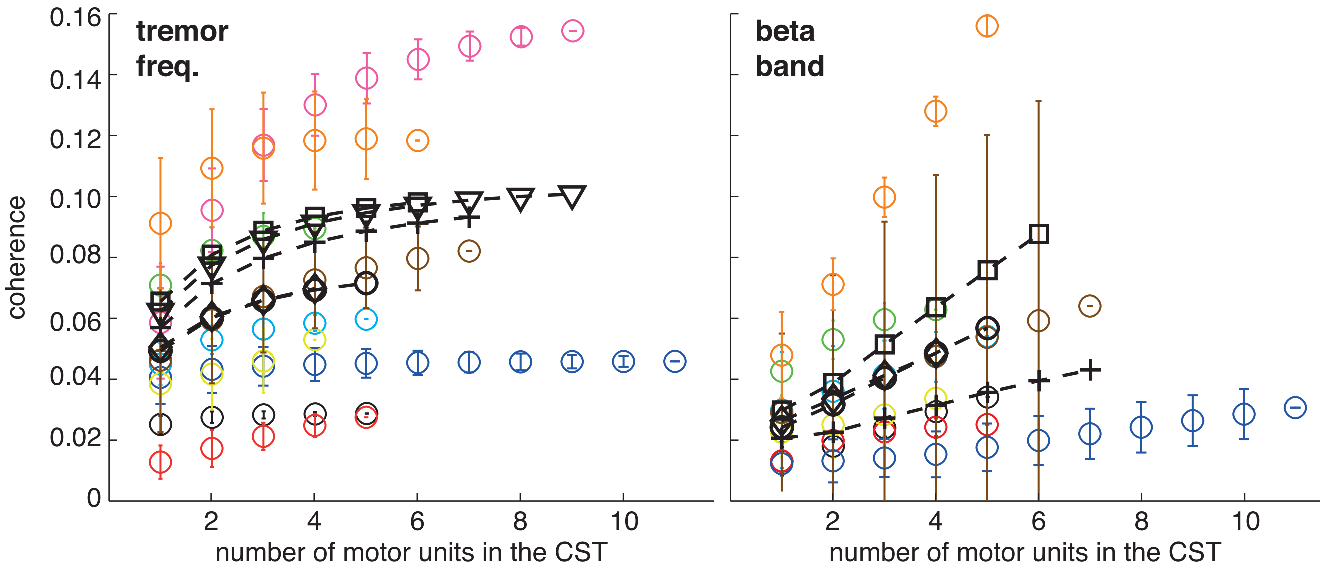
0.16
0.14
0.12
0.10
0.08
0.06
0.04
0.02
0
coherence
tremor
freq.
2
4
6
8
10
number of motor units in the CST
beta
band
2
4
6
8
10
number of motor units in the CST